3D Printed Alumina as a Millimeter-Wave Optical Element

Rex Lam[a], Scott Cray[a], Calvin Firth[a], Shaul Hanany[a], Jürgen Koch[d], Kuniaki Konishi[c], Tomotake Matsumura[b], Yuki Sakurai[b,f], Haruyuki Sakurai[c], Ryota Takaku[e], and Andrew Yan[a]

[a]School of Physics and Astronomy, University of Minnesota, Twin Cities, 115 Union St. SE, Minneapolis MN 55455, USA
[b]Kavli Institute for the Physics and Mathematics of the Universe (IPMU), The University of Tokyo, 5-1-5 Kashiwa-no-Ha, Kashiwa, Chiba 277-8583, Japan
[c]Institute for Photon Science and Technology (IPST), The University of Tokyo, 7-3-1 Hongo, Bunkyo-ku, Tokyo 113-8654, Japan
[d]Laser Zentrum Hannover, Hollerithallee 8 D-30419, Hannover, Germany
[e]Inter-University Research Institute Cooperation High Accelerator Research Organization (KEK) International Center for Quantum-field Measurement Systems for Studies of the Universe and Particles (QUP), 1-1, Oho, Tsukuba, Ibaraki, 305-0801, Japan
[f]Suwa University of Science, 5000-1 Toyohira, Chino-shi, Nagano 391-0292, Japan

ABSTRACT

We present transmission and loss measurements of 3D printed alumina and reflectance measurement of a sample with 3D printed sub-wavelength structures anti-reflection coatings (SWS-ARC). For a band between 160 and 700 GHz we find an index of refraction $n = 3.11 \pm 0.01$ and loss $\tan\delta = 0.002 \pm 0.003$. Transmission measurements between 160 and 250 GHz of a sample with SWS-ARC 3D printed on one side give a reduction of reflectance from a maximum of 64% to a maximum of 31% over the band, closely matching predictions. These first measurements of the index and loss over this frequency band suggest that the material could be useful for astrophysical applications.

Keywords: Alumina, 3D Printed, Transmissivity, Sub-Wavelength Structures, Anti-reflective Coatings, Millimeter-wave Optical components

1. INTRODUCTION

Alumina is a material widely used in millimeter and sub-millimeter wave astrophysics for lenses and sub-millimeter filters. It has among the lowest loss in the millimeter wave band, relatively high absorption in the IR, and high thermal conductance leading to low emission when heat sunk at cryogenic temperatures.[1] This makes it useful as a low-pass filter for use in telescopes.[2–4]

Alumina's high index of refraction $n \simeq 3$[5] requires implementing an anti-reflection coating to avoid large reflections, and several ARC techniques have been proposed.[6–10] Our group has been focused on implementing the technique of sub-wavelength structures (SWS) as an ARC.[2,11–16]

Two methods have been proposed to fabricate SWS on alumina: dicing[17] and laser ablation.[2,13,16,18,19] Due to the hardness of alumina, dicing has been reported to require multiple replacements of blades over optical elements that are tens of cm in diameter.[17] Laser ablation is wear-free, and therefore scalable to large quantities and diameters if ablation rates are demonstrated to be sufficiently high. To date, authors report ablation rates on alumina between 0.5 and 34 mm^3/min,[14,20–22] spanning a variety of ablation conditions including laser type and power, pulse duration, scan speed, etc. The largest laser-ablated alumina optical element that has been laser ablated is 300 mm diameter and is operating with the MUSTANG2 instrument.[2] It took less than 4 days to make, and the reported ablation rate was 18 mm^3/min.[2]

Another method to fabricate alumina is through additive manufacturing. At the millimeter-wave, the properties of 3D-printed alumina have recently been characterized at frequencies between 75 and 110 GHz.[23] Additive manufacturing opens pathways for patterning SWS on either flat or curved alumina samples at the time of optical

Millimeter, Submillimeter, and Far-Infrared Detectors and Instrumentation for Astronomy XII, edited by Jonas Zmuidzinas, Jian-Rong Gao, Proc. of SPIE Vol. 13102, 131022N · © 2024 SPIE · 0277-786X · doi: 10.1117/12.3019180

element fabrication obviating the need for subtractive manufacturing. 3D printing might also give higher aspect ratio SWS.

In this paper we report about the properties of samples of 3D printed alumina without and with SWS-ARC. We describe the samples in Section 2. In Section 3 we give transmission and loss measurements between 160 and 700 GHz of bare 3D-printed alumina, and transmission measurements between 160 and 250 GHz of a sample that had SWS 3D printed on one side. We discuss the results and summarize in Section 4. To our knowledge, these are the first measurements of 3D-printed alumina over this frequency range.

2. SAMPLES

Nishimura*, a company that specializes in sintering alumina powder, partnered with SK FINE†, a company that specializes in 3D printing, to make two alumina discs. One disc, henceforth referred to as 'flat', was 50 mm in diameter, 29.4 ± 0.005 mm thick, and was flat on both sides. A second disc, henceforth referred to as 'patterned', had SWS on one side. A schematic cross section of the patterned sample is shown in Figure 1. We used a confocal microscope to measure the SWS over more than 50 pyramids. A sample image is given Figure 2, and averages and standard deviations of the measurements are given in Table 1.

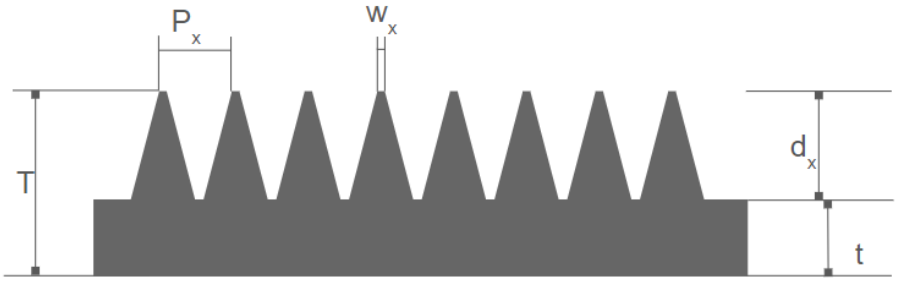

Figure 1. Schematic of a 1D cross section in x of the patterned disc. The schematic is not-to-scale.

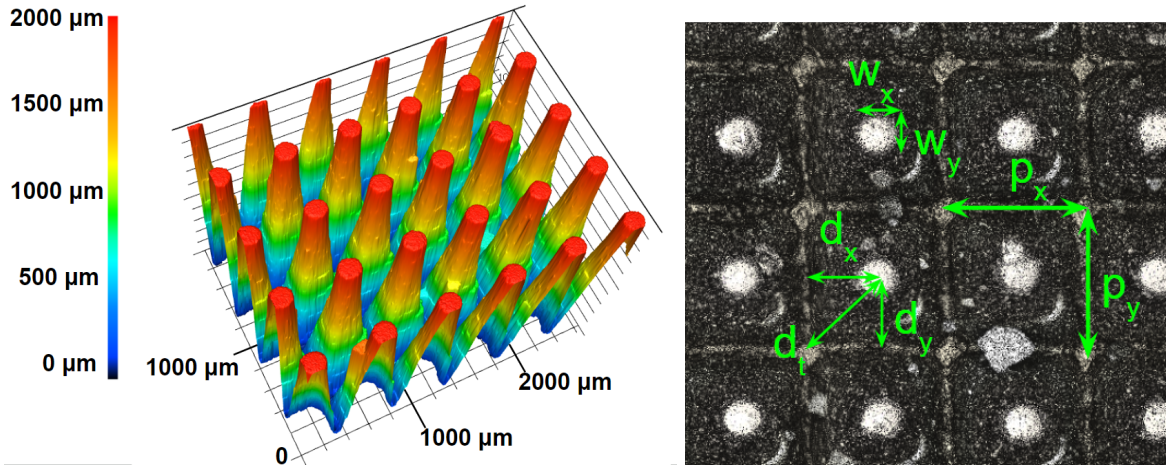

Figure 2. Confocal microscope images of a section of the 3D-printed patterned disc. The right image gives definitions of the shape parameters.

*https://nishimuraac.com/
†https://www.sk-fine.co.jp/en/

Table 1. Parameters of 3D printed alumina with patterned SWS. The parameters are defined in Figure 1 and the right panel of Figure 2. The data are averages over at least 50 pyramids.

Parameter	Measured(mm)
Diameter (D)	40.18 ± 0.05
Total Thickness (T)	2.919 ± 0.007
Thickness of Substrate (t)	1.04 ± 0.01
Pitch x (P_x)	0.495 ± 0.004
Pitch y (P_y)	0.494 ± 0.005
Top Width x(w_x)	0.165 ± 0.005
Top Width y(w_y)	0.155 ± 0.005
Saddle depth x (d_x)	1.88 ± 0.04
Saddle depth y (d_y)	1.87 ± 0.07
Total Depth (d_t)	1.946 ± 0.006

3. MEASUREMENTS

We measured the transmission and reflection of both samples using a vector network analyzer (VNA) and the experimental configurations shown in Figure 3. All measurements were repeated twice to check for reproducibility, and the two were nearly identical. Only a single measurement was used for subsequent data analysis. The transmission and reflection of the flat and patterned discs were conducted over 160 – 700 GHz, and 160 – 260 GHz, respectively, and the data are given in Figures 4 and 5.

The transmission measurement is normalized by a measurement without the sample and the reflection measurement is normalized by comparing the measurement to a measurement with a gold mirror in place of where the sample would be. All raw VNA data are squared to give a measure of power transmittance and reflectance.

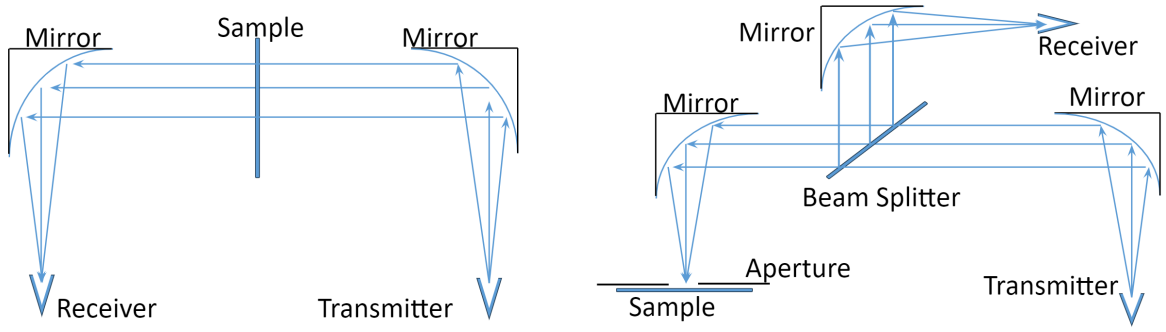

Figure 3. Experimental configurations for transmission (left panel) and reflection measurements (right panel). The 'Transmitter' and 'Receiver' functions are provided by a vector network analyzer. The sketches are not to-scale.

4. ANALYSIS AND RESULTS

4.1 Flat Disc

We least-squares fit the transmission and reflection data of the flat sample to a theoretical model to extract a best-fit index of refraction n and loss tangent $\tan\delta$. These values are given in Table 2. The residual from the best fit is shown in Figure 4 and we use the standard deviation of this residual as a measure of noise in the data. The overall standard deviation of the residual $\sigma = 0.055$ is dominated by the transmission data $\sigma_{\mathrm{T}} = 0.071$. We use σ to produce a reduced χ^2 and to find a range of uncertainty for n and δ for data in each of the incident polarization states. These uncertainties are given in Table 2.

4.2 Patterned Disc

We compare the measurements to theoretical predictions using rigorous coupled-wave analysis (RCWA)[24] assuming the measured geometry given in Table 1 and an index and loss matching the measurements reported in

Table 2. The best-fit index of refraction and loss tangent values including 68% uncertainties for the flat disc sample for each of the incident polarization angles.

Parameter	Value
n	3.11 ± 0.01
δ	0.002 ± 0.003

Table 2. The RCWA-calculated transmittance and reflectance are shown in Figure 5. The RCWA calculation shows the signature of diffraction, which is calculated to set in at frequencies higher than $\nu_{\text{diff}} = c/pn_s = 195$ GHz, where p is the pitch and n_s is the index of refraction.[15]

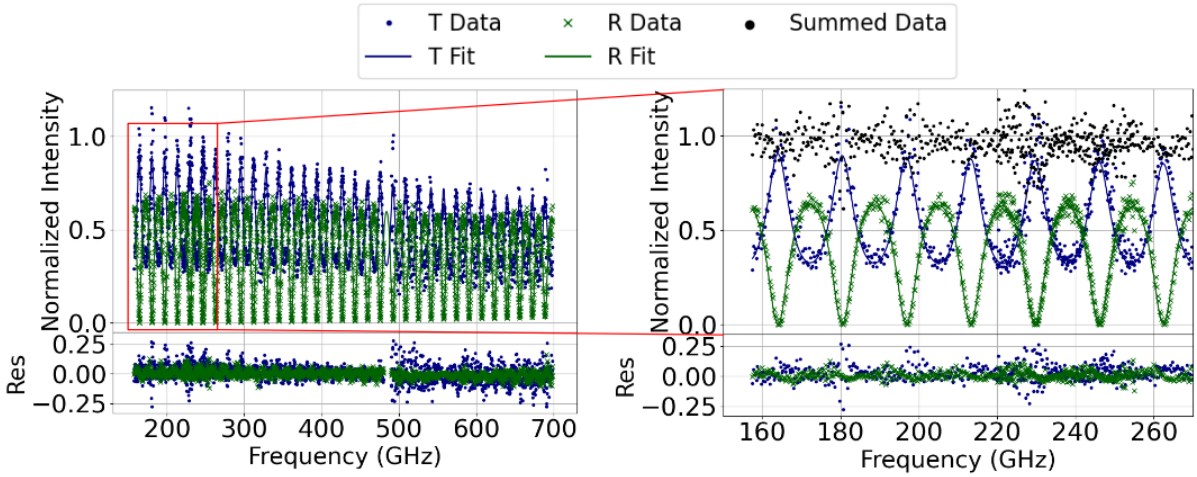

Figure 4. Transmission and reflection data as a function of frequency (upper panels, blue and green dots, respectively) of the flat disc, the best fit models (solid, same colors), and the residuals from the best fits (lower panels). The expanded view of a low frequency band (right panel) also gives the sum of the measured transmission and reflection (black).

The flat disc was measured to have a maximum reflection of 64%. This is reduced to a maximum of 31% with SWS.

5. DISCUSSION AND SUMMARY

A single index of refraction and loss tangent fit the transmission and reflection spectrum of the flat disc over a broad frequency range between 160 and 700 GHz. The value of the index of refraction is close to values measured with standard sintered alumina.[1,2,5] The loss tangent is not constrained well, see Table 2, although the RCWA fit to the transmission data shown in Figure 4, in which we used $\tan\delta = 0.002$ suggests a lower value. Higher precision measurements are required to gauge whether the sample has loss values competitive with standard alumina. For future samples, it would also be important to receive information from vendors quantifying the purity of the 3D-printed material, and the nature of foreign agents.

To our knowledge, these are the first measurements of the optical properties of 3D-printed alumina between 160 and 700 GHz, and the first demonstration of 3D-printed structures as SWS-ARC. The measurements indicate that the approach is promising, and over time the technology could mature from samples that are few cm in diameter to ones with diameters of tens of cm.

ACKNOWLEDGMENTS

We thank Patrick Camilleri for use of the VKX-3000 confocal microscope with which we imaged the patterned alumina. We thank Nick Agladze at ITST/UC Santa Barbara for the transmission and reflection measurements. Portions of this work were conducted in the Minnesota Nano Center, which is supported by the National Science

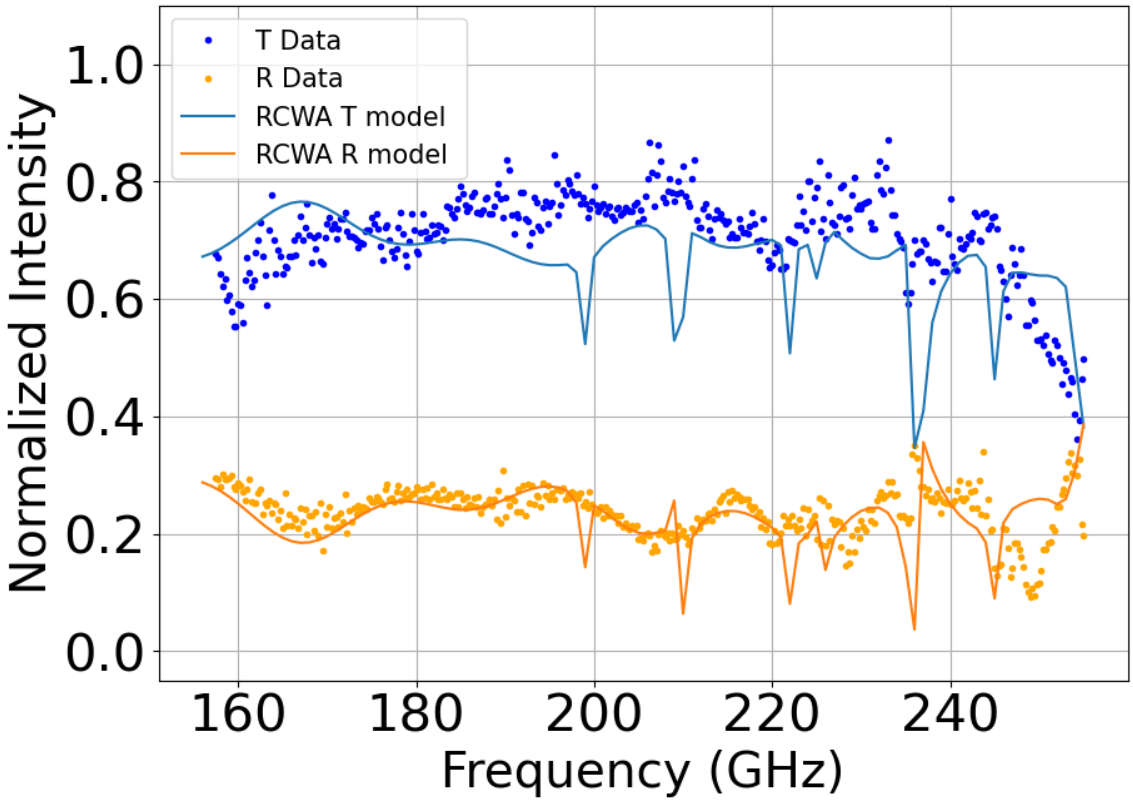

Figure 5. Transmission (blue points) and reflection (orange points) of the patterned disc. The blue and orange lines are the models generated by RCWA given the average geometric parameters of the patterned disc as given in Table 1.

Foundation through the National Nanotechnology Coordinated Infrastructure (NNCI) under Award Number ECCS-2025124. This work was supported by NSF grant number 2206087. This work was supported by JSPS KAKENHI Grant Number JP23H00107, and JSPS Core-to-Core Program, A. Advanced Research Networks. This work was performed in part at the Center for Data-Driven Discovery (CD3), Kavli IPMU (WPI). The Kavli IPMU is supported by World Premier International Research Center Initiative (WPI Initiative), MEXT, Japan. This study was funded in parts by MEXT Quantum Leap Flagship Program (MEXT Q-LEAP, Grant Number JPMXS0118067246).

REFERENCES

[1] Inoue, Y., Matsumura, T., Hazumi, M., Lee, A. T., Okamura, T., Suzuki, A., Tomaru, T., and Yamaguchi, H., "Cryogenic infrared filter made of alumina for use at millimeter wavelength," *Appl. Opt.* **53**, 1727–1733 (Mar 2014).

[2] Takaku, R., Wen, Q., Cray, S., Devlin, M., Dicker, S., Hanany, S., Hasebe, T., Iida, T., Katayama, N., Konishi, K., Kuwata-Gonokami, M., Matsumura, T., Mio, N., Sakurai, H., Sakurai, Y., Yamada, R., and Yumoto, J., "Large diameter millimeter-wave low-pass filter made of alumina with laser ablated anti-reflection coating," *Optics express* **29**(25), 41745–41765 (2021).

[3] Ade, P. A. R., Ahmed, Z., Amiri, M., Barkats, D., Thakur, R. B., Bischoff, C. A., Beck, D., Bock, J. J., Boenish, H., Bullock, E., Buza, V., Cheshire, J. R., I., Connors, J., Cornelison, J., Crumrine, M., Cukierman, A., Denison, E. V., Dierickx, M., Duband, L., Eiben, M., Fatigoni, S., Filippini, J. P., Fliescher, S., Goeckner-Wald, N., Goldfinger, D. C., Grayson, J., Grimes, P., Hall, G., Halal, G., Halpern, M., Hand, E., Harrison, S., Henderson, S., Hildebrandt, S. R., Hilton, G. C., Hubmayr, J., Hui, H., Irwin, K. D., Kang, J., Karkare, K. S., Karpel, E., Kefeli, S., Kernasovskiy, S. A., Kovac, J. M., Kuo, C. L., Lau, K., Leitch, E. M., Lennox, A., Megerian, K. G., Minutolo, L., Moncelsi, L., Nakato, Y., Namikawa, T., Nguyen, H. T., O'Brient, R., Ogburn, R. W., I., Palladino, S., Prouve, T., Pryke, C., Racine, B., Reintsema, C. D., Richter, S., Schillaci, A., Schwarz, R., Schmitt, B. L., Sheehy, C. D., Soliman, A., Germaine, T. S., Steinbach, B., Sudiwala, R. V., Teply, G. P., Thompson, K. L., Tolan, J. E., Tucker, C., Turner, A. D., Umiltà, C., Vergès, C., Vieregg, A. G., Wandui, A., Weber, A. C., Wiebe, D. V., Willmert, J., Wong, C. L., Wu, W. L. K., Yang, H., Yoon, K. W., Young, E., Yu, C., Zeng, L., Zhang, C., and Zhang, S., "BICEP/Keck XV: The BICEP3 Cosmic Microwave Background Polarimeter and the First Three-year Data Set," *Astrophysical Journal* **927**, 77 (Mar. 2022).

[4] Golec, J. E., Sutariya, S., Jackson, R., Zimmerman, J., Dicker, S. R., Iuliano, J., McMahon, J., Puglisi, G., Tucker, C., and Wollack, E. J., "Simons observatory: broadband metamaterial antireflection cuttings for large-aperture alumina optics," *Appl. Opt.* **61**, 8904–8911 (Oct 2022).

[5] Lamb, J. W., "Miscellaneous data on materials for millimetre and submillimetre optics," *Int. J. Infrared Millimeter Waves* **17**, 1997–2034 (Dec. 1996).

[6] Nadolski, A., Kofman, A. M., Vieira, J. D., Ade, P. A. R., Ahmed, Z., Anderson, A. J., Avva, J. S., Thakur, R. B., Bender, A. N., Benson, B. A., Carlstrom, J. E., Carter, F. W., Cecil, T. W., Chang, C. L., Cliche, J. F., Cukierman, A., de Haan, T., Ding, J., Dobbs, M. A., Dutcher, D., Everett, W., Foster, A., Fu, J., Gallichio, J., Gilbert, A., Groh, J. C., Guns, S. T., Guyser, R., Halverson, N. W., Harke-Hosemann, A. H., Harrington, N. L., Henning, J. W., Holzapfel, W. L., Huang, N., Irwin, K. D., Jeong, O. B., Jonas, M., Jones, A., Khaire, T. S., Korman, M., Kubik, D. L., Kuhlmann, S., Kuo, C.-L., Lee, A. T., Lowitz, A. E., Meyer, S. S., Michalik, D., Montgomery, J., Natoli, T., Nguyen, H., Noble, G. I., Novosad, V., Padin, S., Pan, Z., Pearson, J., Posada, C. M., Quan, W., Rahlin, A., Ruhl, J. E., Sayre, J. T., Shirokoff, E., Smecher, G., Sobrin, J. A., Stark, A. A., Story, K. T., Suzuki, A., Thompson, K. L., Tucker, C., Vanderlinde, K., Wang, G., Whitehorn, N., Yefremenko, V., Yoon, K. W., and Young, M. R., "Broadband anti-reflective coatings for cosmic microwave background experiments," in [*Millimeter, Submillimeter, and Far-Infrared Detectors and Instrumentation for Astronomy IX*], Zmuidzinas, J. and Gao, J.-R., eds., **10708**, 1070843, International Society for Optics and Photonics, SPIE (2018).

[7] Groh, J. C., *Design and Deployment of the Simons Array Cosmic Microwave Background Polarization Instrument*, PhD thesis, University of California, Berkeley (Jan. 2021).

[8] Priyadarshini, B. G. and Sharma, A. K., "Design of multi-layer anti-reflection coating for terrestrial solar panel glass," *Bull. Mater. Sci. (India)* **39**, 683–689 (June 2016).

[9] Askar, K., Phillips, B. M., Fang, Y., Choi, B., Gozubenli, N., Jiang, P., and Jiang, B., "Self-assembled self-cleaning broadband anti-reflection coatings," *Colloids Surf. A Physicochem. Eng. Asp.* **439**, 84–100 (Dec. 2013).

[10] Chao, Y.-C., Chen, C.-Y., Lin, C.-A., and He, J.-H., "Light scattering by nanostructured anti-reflection coatings," *Energy Environ. Sci.* **4**(9), 3436 (2011).

[11] Rytov, S., "Electromagnetic properties of a finely stratified medium," *Soviet Physics JEPT* **2**, 466–475 (1956).

[12] Raut, H. K., Ganesh, V. A., Nair, A. S., and Ramakrishna, S., "Anti-reflective coatings: A critical, in-depth review," *Energy Environ. Sci.* **4**(10), 3779 (2011).

[13] Matsumura, T., Young, K., Wen, Q., Hanany, S., Ishino, H., Inoue, Y., Hazumi, M., Koch, J., Suttman, O., , and Schütz, V., "Millimeter-wave broadband antireflection coatings using laser ablation of subwavelength structures," *Appl. Opt.* **55**, 3502–3509 (May 2016).

[14] Wen, Q., Fadeeva, E., Hanany, S., Koch, J., Matsumura, T., Takaku, R., and Young, K., "Picosecond laser ablation of millimeter-wave subwavelength structures on alumina and sapphire," *Optics & Laser Technology* **142**, 107207 (2021).

[15] Takaku, R., Hanany, S., Imada, H., Ishino, H., Katayama, N., Komatsu, K., Konishi, K., Kuwata-Gonokami, M., Matsumura, T., Mitsuda, K., Sakurai, H., Sakurai, Y., Wen, Q., Yamasaki, N. Y., Young, K., and Yumoto, J., "Broadband, millimeter-wave anti-reflective structures on sapphire ablated with femto-second laser," *Journal of Applied Physics* **128**(22), 225302 (2020).

[16] Schütz, V., Young, K., Matsumura, T., Hanany, S., Koch, J., Suttmann, O., Overmeyer, L., and Wen, Q., "Laser processing of sub-wavelength structures on sapphire and alumina for millimeter wavelength broadband anti-reflection coatings," *Journal of Laser Micro Nanoengineering* **11**, 204–209 (01 2016).

[17] Golec, J. E., McMahon, J. J., Ali, A. M., Chesmore, G. E., Cooperrider, L., Dicker, S., Galitzki, N., Harrington, K., Jackson, R., Westbrook, B., Wollack, E. J., Xu, Z., and Zhu, N., "Design and fabrication of metamaterial anti-reflection coatings for the Simons Observatory," in [*Advances in Optical and Mechanical Technologies for Telescopes and Instrumentation IV*], Navarro, R. and Geyl, R., eds., **11451**, 114515T, International Society for Optics and Photonics, SPIE (2020).

[18] Öktem, B., Pavlov, I., Ilday, S., Kalaycıoğlu, H., Rybak, A., Yavaş, S., Erdoğan, M., and Ilday, F. Ö., "Nonlinear laser lithography for indefinitely large-area nanostructuring with femtosecond pulses," *Nat. Photonics* **7**, 897–901 (Nov. 2013).

[19] Wang, L., Cao, X.-W., Lv, C., Xia, H., Tian, W.-J., Chen, Q.-D., Juodkazis, S., and Sun, H.-B., "Formation of deep-subwavelength structures on organic materials by femtosecond laser ablation," *IEEE Journal of Quantum Electronics* **54**(1), 1–7 (2018).

[20] Furmanski, J., Rubenchik, A. M., Shirk, M. D., and Stuart, B. C., "Deterministic processing of alumina with ultrashort laser pulses," *J. Appl. Phys.* **102**, 073112 (Oct. 2007).

[21] Perrie, W., Rushton, A., Gill, M., Fox, P., and O'Neill, W., "Femtosecond laser micro-structuring of alumina ceramic," *Appl. Surf. Sci.* **248**, 213–217 (July 2005).

[22] Beausoleil, C., Yazdani Sarvestani, H., Katz, Z., Gholipour, J., and Ashrafi, B., "Deep and high precision cutting of alumina ceramics by picosecond laser," *Ceram. Int.* **46**, 15285–15296 (July 2020).

[23] Jiménez-Sáez, A., Schüßler, M., Krause, C., Pandel, D., Rezer, K., Vom Bögel, G., Benson, N., and Jakoby, R., "3d printed alumina for low-loss millimeter wave components.," *IEEE Access* **7**(8679963), 40719 (2019).

[24] M.G. Moharam, E.B. Grann, D.A. Pommet, T.K. Gaylord, "Formulation for stable and efficient implementation of the rigorous coupled-wave analysis of binary gratings," *J. Opt. Soc. Am. A* **12**(5), 1068–1076 (1995).